MARS OBSERVER 1NTERPLANETAR% CRUISE ORBIT DETERMINATION

L. A. Cangahuala, E. J. Graat*, D. C. Roth, S. W. Demcak†, P. B. Esposito, R. A. Mase

Navigation Systems Section, Jet Propulsion Laboratory
California Institute of Technology, Pasadena,CA91109-8099

The Mars Observer orbit determination activity extending from launch to loss of contact is summarized, and includes quantitative results and conclusions derived from mission experience. The major topics include (i) a description of the relevant orbit determination models, (ii) an identification and quantification of the major orbit determination error sources, (iii) a review of salient orbit determination results, with emphasis on the Mars approach phase orbit determination, and (iv) a comparison of predicted versus actual orbit determination performance. Special emphasis is given to the consistency of the orbit determination results across different radiomet ric observation type combinations and data arc lengths.

The Mars Observer (MO) interplanetary cruise phase lasted eleven months, starting 25 September 1992. The final confirmed receipt of radiometric tracking data was on 22 August 1993, less than three days before the planned Mars Orbit Insertion (MO]) maneuver. During the interplanetary cruise to Mars. the MO navigation team's orbit determination analysts determined the spacecraft's trajectory, provided orbit determination solutions for maneuver designs and on-board spacecraft ephemerides, and assessed the quality and effectiveness of the navigation models and tracking data,

Orbit determination models are introduced in the following categories: (i) measurement observable, (ii) spacecraft dynamics, (iii) geodetic models, and (iv) filter models. Attention is given to the radiometric data quality and Mars encounter estimates and uncertainties throughout the cruise. The salient orbit determination history is presented, leading up to the solutions selected for the backup and final MOI maneuver designs. The solution submitted for the backup MO] design, created 60 days before encounter, exemplified the consistency of the MO orbit determination results. This solution was found to be within 0.6 km and 1 mm/s in radial distance and velocity, respective y, to the orbit reconstructi on. In addition, orbit determination solutions created with different radiometric observation type combinations and data arc lengths were in agreement during the entire cruise. Finally, the predicted versus actual orbit determinant ion performance is presented.

INTRODUCTION

The Mars Observer Spacecraft was launched on a Titan III booster on 25 September 1992. The final receipt of tracking data from the spacecraft took pl ace on 22 August 1993, three days before the planned Mars Orbit Insertion (MOI) maneuver was to have taken place (for a comprehensive description of the mission, see Reference [1]). During the eleven month cruise, three trajectory correct ion maneuvers (TCMs) and MOI were designed by the navigation team. The orbit determination analysts, using three different radiometric data types (2-way X-band Doppler & range, and Doubly-Differenced One Way Range (ADOR)), reconstructed the TCMs, and gained insight into the spacecraft dynamics and efficacy of the modeling. This paper describes these insights as well as the orbit determination history and accuracy, to emphasize the importance of good modeling to future orbit determination analysts.

*Sterling Soft ware, Pasadena, CA
†OAO Corporation, Altadena, CA

The basic procedure for reconstructing and predicting the MO position and velocity throughout cruise was through weighted least-squares differential corrections to a mathematical model. The first section of this paper describes those models whose effectiveness (or limitations) were revealed during cruise operations. This section concludes with a table which depicts (i) the *a priori* and estimate uncertainties, and (ii) additional model parameters whose uncertainties were incorporated into the weighted least squares analysis, but whose corrections were not estimated*.

To generate these differential corrections, computed observable were compared to their actual radiometric counterparts. Eleven months of tracking data and three radi omet ric data types made solutions of many different of durations and data type combinations possible. The second section of the paper displays the consistency of these solutions, and the ability of the orbit determination analysts to predict the MO arrival state.

This paper summarizes the final report presented by the orbit determination analysts to the Mars Observer project (Reference 2). For more details about specific models incorporated into the orbit determination process, the reader is directed to Reference 3.

MODELS

Orbit determination models have a wide variety of origins and are not easily organized into a concise set of distinct groups. Some models can be practically identical for every interplanetary mission, while some must be tailored for a specific spacecraft. Regardless of their origins or the motivation for their development, orbit determination models of interest used during the MO cruise are categorized in Table 1.

Table 1: MARS OBSERVER ORBIT DETERMINATION MODEL ORGANIZATION

Model Category	Examples
Observable	Spacecraft rotation, spacecraft signal delays
Spacecraft Dynamics	Solar Radiation Pressure, angular momentum desaturations, non-grav. accelerations
Geodetic Models	Earth rotation and orientation, media delays
Filter Models	Models which provide *a priori* knowledge to the estimation process

The observable models are those which change the physical path length of the two-way signal without changing the location of the spacecraft center of mass (for brevity, unless noted otherwise, all two-way coherent Doppler and range data will hereafter be referred to as simply 'Doppler' and 'range' data). Non-gravitational changes to the spacecraft center of mass location are modeled in the 'spacecraft dynamics' category. The models which affect the ground stat ion location and signal path environment are di scussed under the heading of 'geodetic' models, while all other models associated with the estimation process are described as 'filter' models.

Observable Models

*Spacecraft **Rotation**.* During interplanetary cruise, the MO spacecraft rotated about an axis normal to its solar power array with a 100 minute period. This motion, referred to as Array Normal Spin (ANS), impressed biases and sinusoidal signatures onto the line-of-sight observable (see Figure 1).

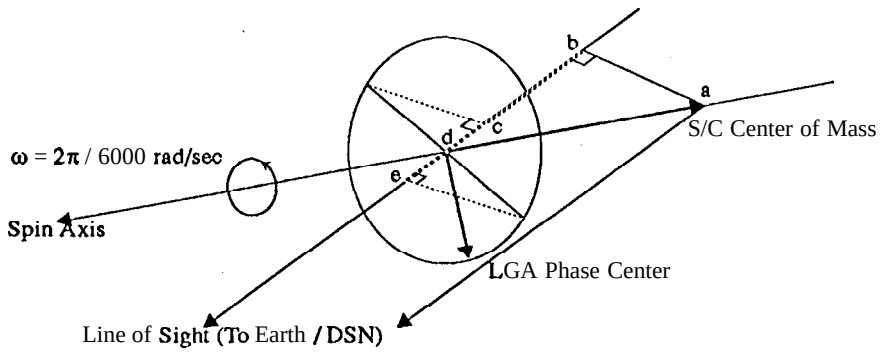

Figure 1: Low Gain Antenna (LGA) Motion Due to Spacecraft Rotation (not to scale)

*These parameters are considered part of the consider analysis.

The Low Gain Antenna (LGA) phase center traced out a circle normal to the spin axis. The intersection of the plane of this circle with the spin axis is offset from the spacecraft center of mass. Therefore, in the line of sight direction, the range data is biased by the distance, *bd,* and oscillates between the points e and c. This oscillation also contributed to the observed sinusoidal signature in the Doppler data residuals. During MO Inner cruise*, the distance of the LGA phase center from the spin axis was 2.1 m. The offset from the center of mass (segment *ad) was 0.83* m.

The magnitude of the Doppler and range oscillations and range bias changed with the orientation of the spin axis with respect to the line of sight†. Since it was difficult to get spin orientation information, the data residuals were used to estimate the spin parameters (spin period (T), projected distance (r'), and phase offset (ϕ)), using Equation 1 as a description of the line-of-sight projection of the ANS velocity (V_{ANS}):

$$v_{ANS} = (2\pi/T)\, r' \cos\,(2\pi t_i/T + \phi) \qquad (1)$$

The noise in the range data (approximately 1-3 meters) was greater than the spin motion described here (on the order of 1 meter); thus, only the Doppler data was used to estimate the spin parameters. Trigonometric and bias adjustments were then calculated for both Doppler and range data in 24 h batches. Figure 2 shows the estimated spin period and uncertainty for consecutive 24 h periods'. Table 2 summarizes the adjustments made to the range and Doppler observable due to ANS. Figures 3a-b demonstrate the dramatic improvement in the post-tit residuals after the application of the trigonometric corrections to the five final days of a solution.

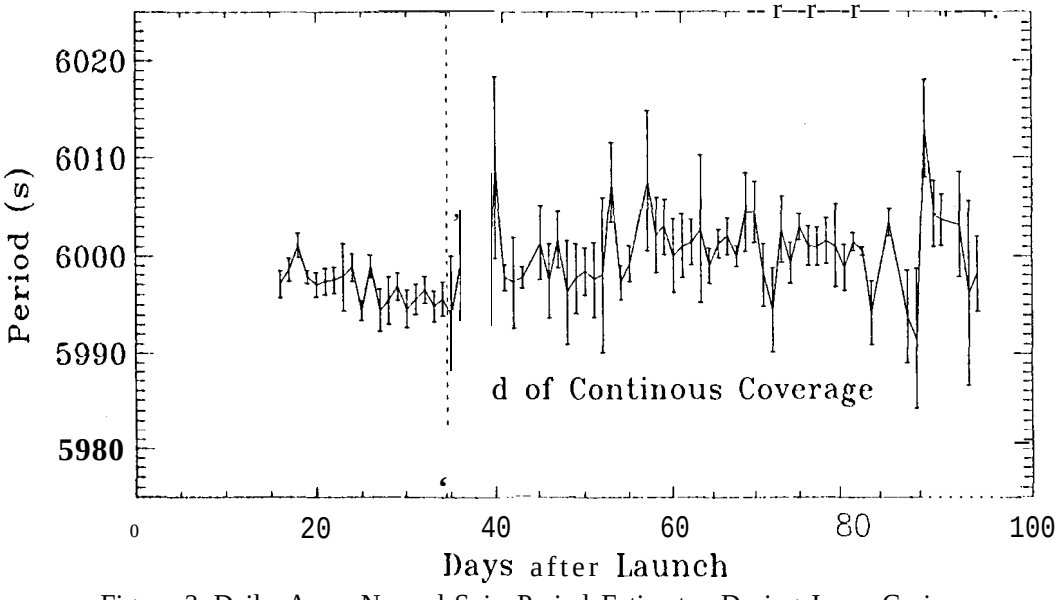

Figure *2:* Daily Array-Normal-Spin Period Estimates During Inner Cruise

Table 2: OBSERVABLE ADJUSTMENTS DUE TO SPACECRAFT ROTATION

Cruise Phase	Antenna Used	Angle Between Spin Axis & Line of Sight (deg)	Doppler Bias (mHz)	Sinusoidal Doppler Signature Magnitude (mHz)	Range Bias (m)	Sinusoidat Range Signature Magnitude (m)
Inner	LGA	Varying	+0.362	Oto 100	0 to +0.83	0 to 2.1
Outer	HGA	~0	+0.362	none	+0.83	none

*The cruise was separated into two phases: Inner and Outer cruise. The Inner cruise period extended from launch (25 September 1992) to 7 January 1993 and was characterized by communication via the LGA and multiple spacecraft attitude changes intended to meet power, thermal, and communication constraints. During the Outer cruise period (7 January 1993 to loss of signal on 22 August 1993) communication was via the HGA.

†The Doppler bias was due to the circularly polarized signal used to communicate with the rotating MO. This bias was constant throughout the cruise.

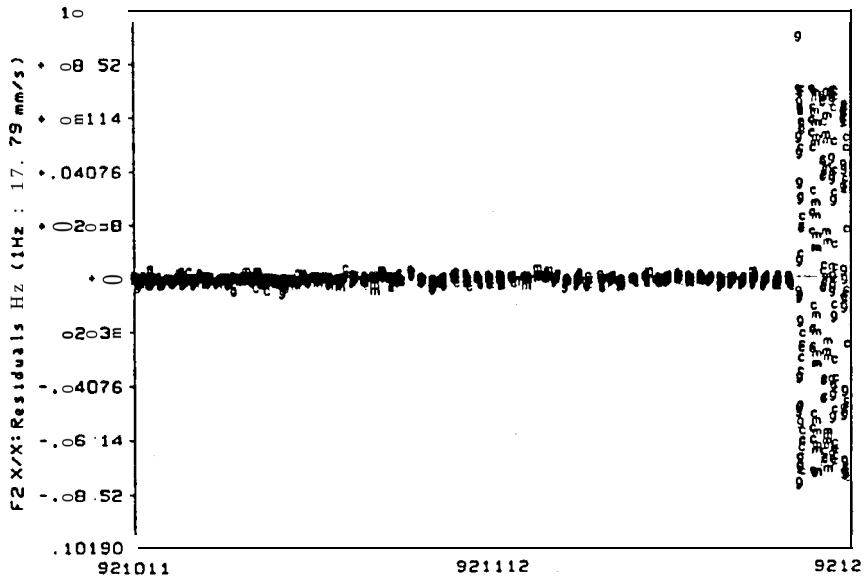

Figure 3a: Doppler Post-Fit Residuals Before Trigonometric Corrections*

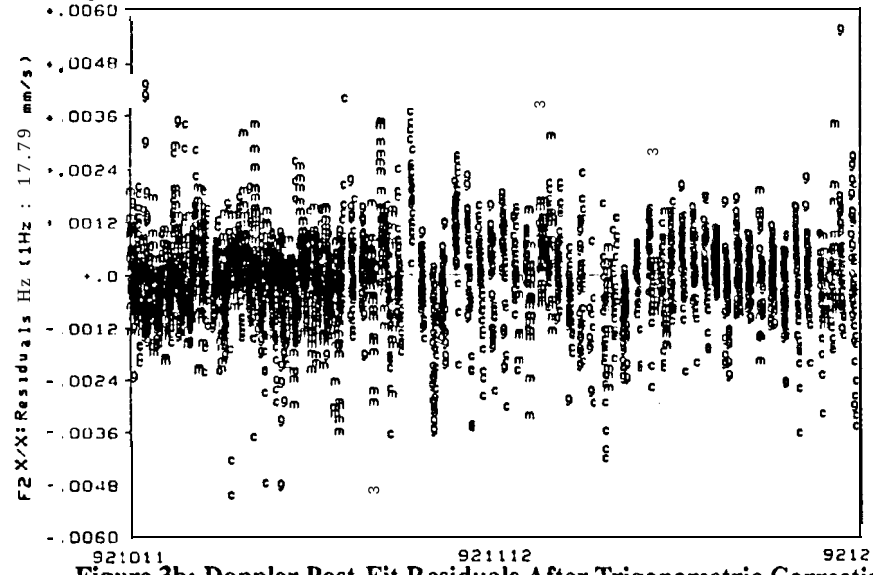

Figure 3b: Doppler Post-Fit Residuals After Trigonometric Corrections

Spacecraft Signal Delay. During the transition from Inner cruise to Outer cruise the High Gain Antenna (HGA) replaced the LGA as the primary communication link. This event took place on 7 January 1993 at 2300 UTC, during a Canberra station pass. Due to an uncompensated change in the signal path length throughout the spacecraft, this transition appeared as a 59.3 range unit (8.5 m) bias in the range residuals (see Figure 4). A corresponding adjustment was made to compensate for this additional delay.

This event gave a measurement of the relative change in path length, accurate to the decimeter (~ 1 range unit) level. This transition was modeled by the DSN as an 8.4 range unit (1.2 m) change according to signal delay measurements made before launch. However, the LGA-HGA signal delay measurements were performed under different conditions. Therefore, the values cited as the absolute signal delay due to spacecraft hardware are considered accurate only to the 60 range unit level at best.

*The residual plot symbols 'g,' 'c,' and 'm' (and '1,' '4,' and '6') refer to residuals from DSN tracking stations at Goldstone, Canberra, and Madrid, respectively.

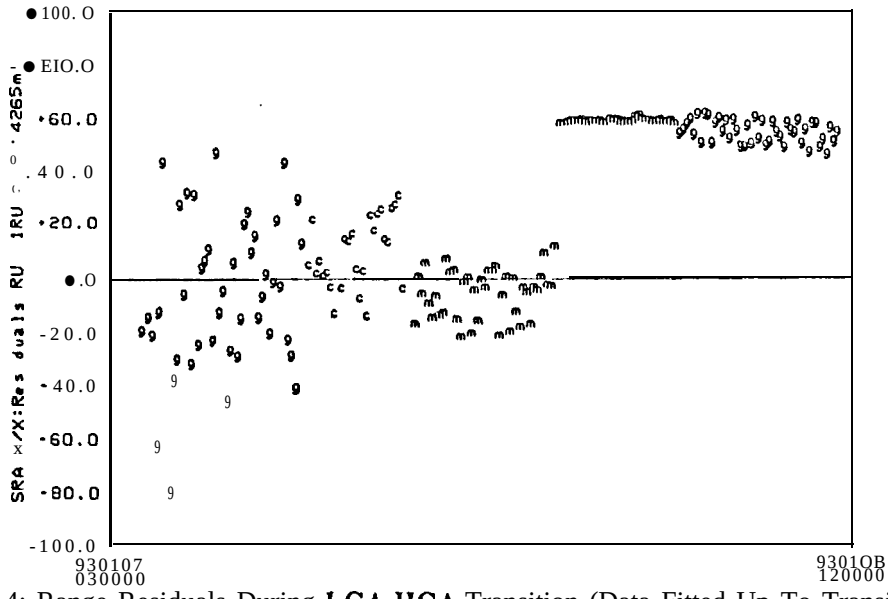

Figure 4: Range Residuals During LGA-HGA Transition (Data Fitted Up To Transition Event)

Spacecraft Dynamic Models

Solar *Radiation Pressure Model. The solar* radiation pressure acceleration model developed for the Mars Observer interplanetary cruise consisted of a self-shadowing parabolic dish and five flat plates. Each of these components were affixed normal to an axis in the spacecraft coordinate system (X, Y, Z) and could be oriented with respect to the sun as a single group. The MO spacecraft coordinate system and major equipment sections are illustrated in Figure 5 for the cruise configurat ion*. The parabolic dish modeled the HGA and was pointed along the spacecraft's +Y axis (the ANS axis). Two flat plates directed along the spacecraft +Y axis were used to model the solar power array. These two components were needed to properly represent the array's active and folded segments which had different reflective properties. The three remaining flat plates were affixed to the spacecraft's +X, +Y, and +Z axes to model the MO instrument bus. Each component had specular and diffuse reflectivity coefficients, μ and v. Diffuse reflectivity imparts an acceleration in the direction normal to the reflecting surface, while the specular term imparts accelerations both normal to and in the plane of the reflecting surface. The component dimensions and reflectivity properties were calculated from spacecraft manufacturer data. Table 3 summarizes the physical properties of each component.

The orientation of each component with respect to the sun was dependent on MO's progress along its interplanetary cruise trajectory. During Inner cruise, the spacecraft's +Y axis was to lie in either the Earth-spacecraft-sun plane or the ecliptic plane and was off-pointed from the sun toward the Earth by an angle which varied between 65.0° and 28.5°. Also, from 2 December 1992 to 30 December 1992, the spacecraft +Y axis was pointed along a series of four inertial vectors in the EME2000 system. These vectors would change by --1° per day during this period. During the Outer cruise period the spacecraft +Y axis pointed Earthward.

In addition to these nominal cruise attitudes, eleven unscheduled, or contingency mode, attitudes were modeled. The particular spacecraft attitude depended on whether the contingency mode occurred during Inner or Outer cruise. For the six Inner cruise contingency modes, the +Y axis was off-pointed from the sun by 65.0° before 2 December 1992 and 55.0° after. The five Outer cruise contingency modes turned the +Y axis directly toward the sun.

At launch, 10 distinct attitudes were thought to be sufficient to model MO's interplanetary cruise. However, by the end of cruise, 62 different attitudes had been modeled. Figure 6a depicts the +Y Axis offset from the sun during Inner cruise, and Figure 6b shows the regimes of +Y Axis Sun and Earth pointing during Outer cruise.

*Figure 5 depicts the spacecraft in its intended cruise configuration. During cruise. the HGA was not fully extended on the boom. so that the dish itself was one dish diameter closer to the MO bus.

Table 3: SOLAR RADIATION PRESSURE ACCELERATION MODEL COMPONENTS

Component	μ	σ_μ	v	σ_v	Dimensions
High-Gain Antenna: Front	0.290	0.030	0.040	0.007	Radius: 0.749 m
Back	o.155	0.020	0.090	0.010	Depth: 0.256 m
Active Solar Array	0.103	0.010	0.037	0.003	16.30 m^2
"Matte" Folded Solar Array	o	-	0.017	0.017	4.10 m^2
+X Bus	0.155	0.020	0.090	0,010	2.72 m^2
+Y Bus	0.155	0.020	0.090	0.010	0.45 m^2
+Z BUS	0.155	0.020	0.090	0.010	3.59 m^2

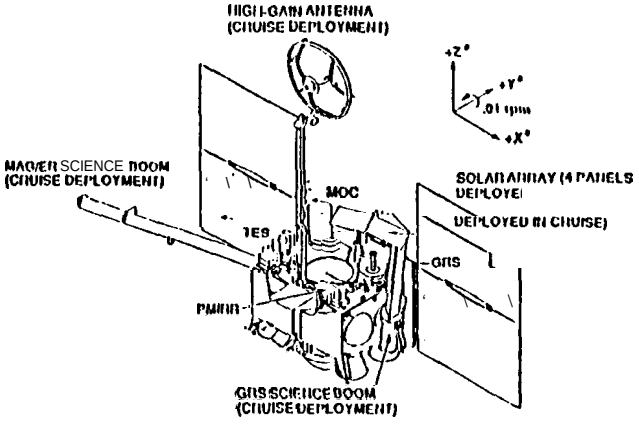

Figure 5: Mars Observer Spacecraft and Spacecraft Fixed Coordinate System

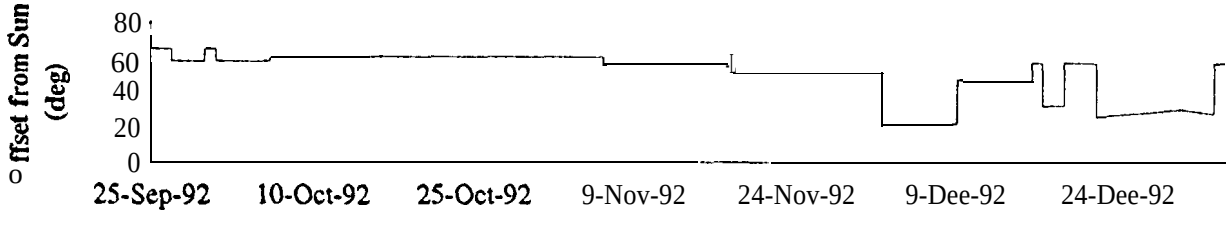

Figure 6a: **+Y** Axis Offset From the Sun During Inner Cruise

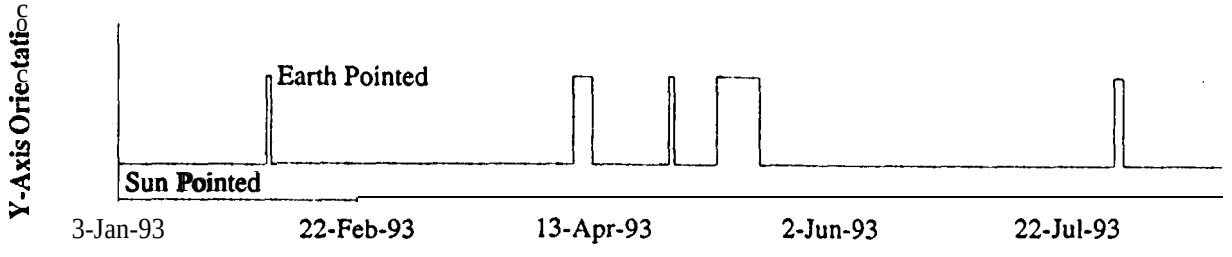

Figure 6b: **+Y** Axis Pointing History During Outer Cruise

Angular Momentum Desaturations. Mars Observer performed 90 angular momentum desaturations (AMDs) to the momentum wheels during interplanetary cruise. These AMDs were performed with a series of short pulse firings of the appropriate spacecraft thruster pairs. The MO spacecraft team supplied the navigation team with data which could be used to reconstruct the AMDs. Two caveats came with this information. First, the AMD event time was only well known when the spacecraft was in coverage by the DSN or when the event was recorded. When an AMD took place outside a tracking pass and was not recorded (as it did for 27 events), the spacecraft team would provide their best estimate of the AMD event time. Since AMD events were correlated to the spacecraft attitude with respect to the sun, these proposed AMD times had a modulo 100 minute (one spin period) uncertainty attached to them. Second, mismatches between balanced thruster pairs were much larger than anticipated. Pre-launch measurements of thruster orientation angles and impulses led to effective AV predictions of less than 0.01 mm/s per desaturation event. During cruise, however, AV'S imparted by each AMD event were observed to be at least an order of magnitude larger than the predicted values. As a result of these limitations, the MO orbit determination analysts devised procedures to ensure that AMDs were well modeled in epoch and component magnitudes.

AMD Epoch Reconstruction. The following demonstrates AMD epoch reconstruction from radiometric tracking data. An AMD event occurred during the tracking gap between 30 October 199220:30 UTC and 31 October 199209:30 UTC. Since the AMD event was not recorded for later playback, no spacecraft team information was provided. The orbit determination analysts used the following procedure to reconstruct the AMD AV and start time:

(1) Determine the AMD's AV by fitting on] y the Doppler tracking data, The instantaneous bum model in the navigation software was used to estimate the AV components. Since the AMD start time was unknown, 31 October 02:00 UTC, SCET was selected as an initial guess. Figure 7a shows the pre-fit Doppler residuals before and after the AMD event. The line-of-sight AV is 0.9553 mm/s and the AMD slowed the spacecraft in the line-of-sight.

(2) Pass the range data through a converged Doppler-only solution. Figure 7b shows the range residuals before and after the AMD event. The range data residuals after the event are biased by 24.25 m (170 range units). This bias is due to the incorrect AMD start time. Since the bias is positive and the AMD was seen to have slowed the spacecraft, the AMD was executed later than assumed.

(3) Calculate the correction to the AMD start time by dividing the bias in the SRA residuals by the line-of-sight ΔV:

$$(24250 \text{ mm}) / (0.9553 \text{ mm/s}) = 25385\text{s}$$

The corrected AMD start time is 31 October 199209:03:05 UTC, SCET. Figure 7c shows the range residuals before and after the AMD using the AV estimated in the Doppler solution and the new start time calculated from the range residual bias. The range residuals show no bias with the corrected start time.

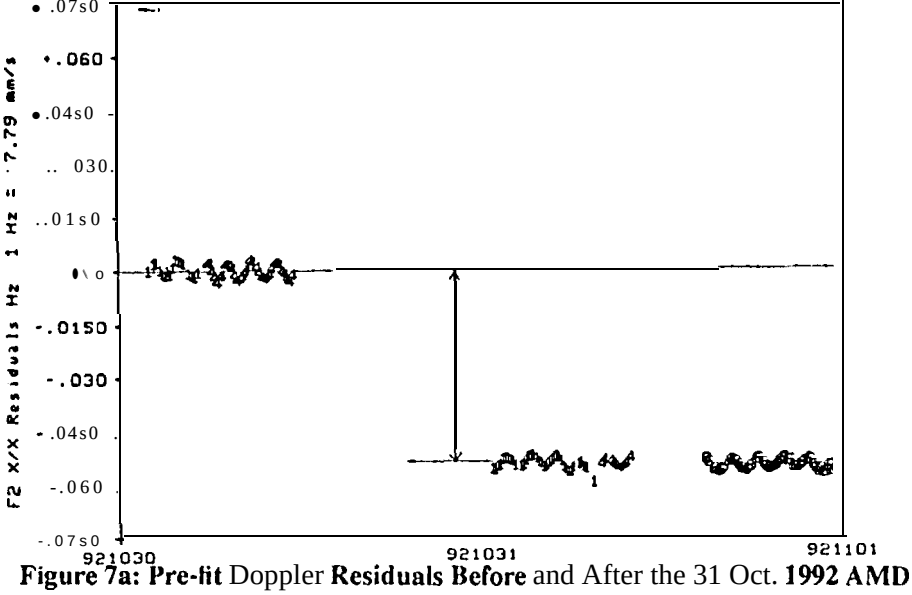

Figure 7a: Pre-fit Doppler **Residuals Before** and After the 31 Oct. **1992 AMD**

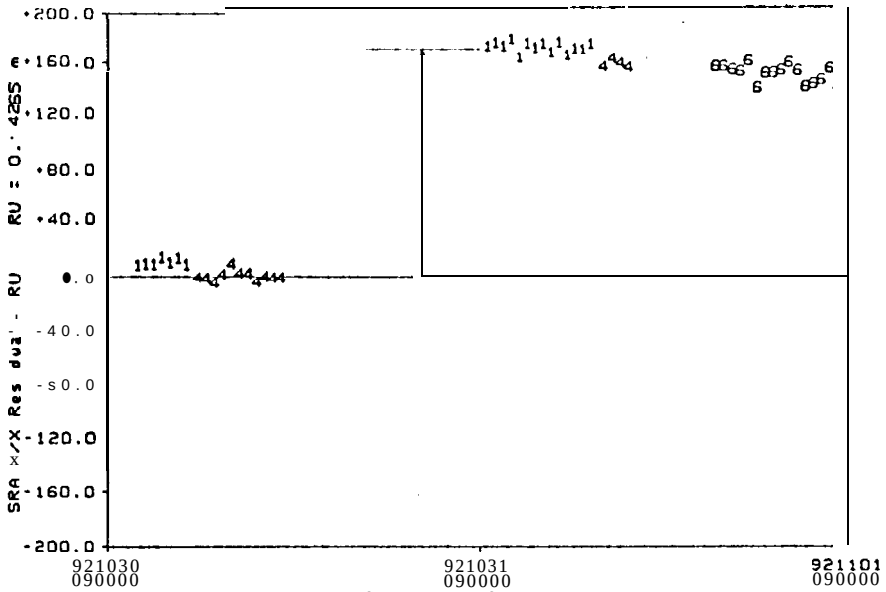

Figure 7b: **Pre-fit Range** Residuals Before and After the 31 Oct. 1992 AMD **(02:00:00 Epoch)**

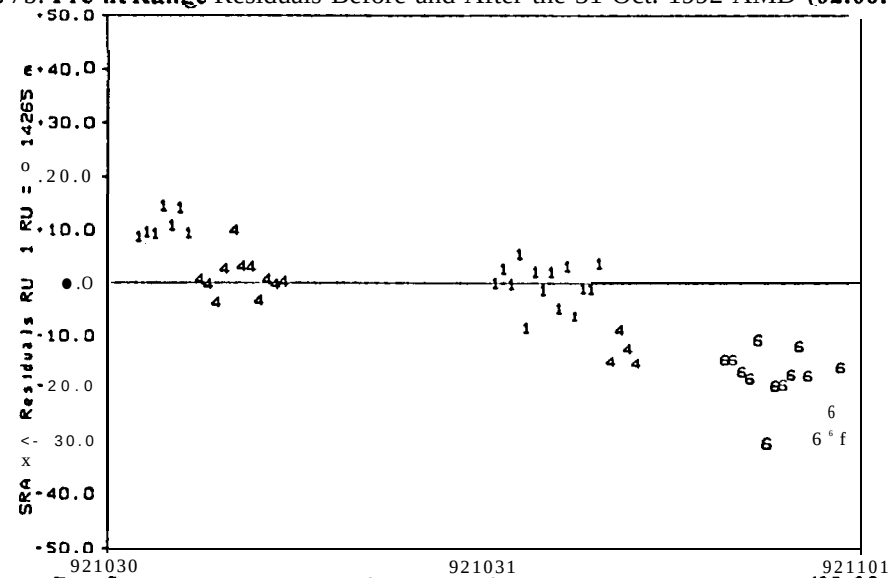

Figure 7c: **Pre-fit** Range Residuals Before and After the 31 Oct. 1992 AMD **(09:03:05** Epoch)

AMD Component Reconstruction. Anticipating potential difficulties in estimating AMD AVS during the Mars orbit insertion and mapping phases, the navigation team attempted to calibrate the thrust per pulse values for each thruster pair, in the hope of improving the modeling of these events. During Outer cruise, a procedure was developed to reconstruct AMD components using line-of-sight information from the Doppler data and spacecraft orientation information. AMD AV'S were initially estimated in J2000 coordinates, rotated into spacecraft-centered spacecraft-fixed coordinates, then normalized into AV per thruster pulse values for each AMD component. For common thruster pairs, normalized AV'S along the spacecraft-fixed Y axis ($|\Delta V_{y\text{-}s/c}|$) demonstrated consistency for AMD events during Outer cruise (Inner cruise AMD AV events were not well estimated due to the difficulty in rotating any spacecraft-centered axis to the Iine-of-sight direction). The $|\Delta V_{y\text{-}s/c}|$ estimates had uncertainties of around 10 mm/s. As a result, the best determined $|\Delta V_{y\text{-}s/c}|$ for each thruster set was chosen to scale all AMD's using that particular thruster set. Using the representative values of $|\Delta V_{y\text{-}s/c}|$ and the number of pulses for each AMD event, the total AV per AMD along the spacecraft Y-axis ($\Delta V_{y\text{-}s/c}$) was reconstructed for Inner and Outer cruise AMD's.

Reconstructed $\Delta V_{y\text{-}s/c}$ values were input to the navigation software. As these values were deemed to be very good estimates, they were *not* re-estimated. Instead, only the less well determined plane-of-sky X and Z components of AV were re-estimated. The a *priori* uncertainty was maintained at 1.0 mm/s, as in the original estimate. These newly estimated AV components were rotated, normalized, and compared to the initial estimated, normalized values, to determine if this reconstruction yielded more realistic values of the total AV per AMD event.

Three signs indicate that this reconstruction yielded more realistic values of the total AV per AMD. First, Doppler, range, and ADOR residual statistics improved slightly. Second, the scatter of the normalized ΔV- X and Z components ($|\Delta V_{x\text{-}sc}|$ and $|\Delta V_{z\text{-}sc}|$, respectively) was significantly reduced. Third, the final estimated vatues of $|\Delta V_{x\text{-}sc}|$ and $|\Delta V_{z\text{-}sc}|$ were, for the most part, much more consistent with the well determined values of $|\Delta V_{y\text{-}sc}|$.

Non-gravitational Forces. The orbit determination analysts found that the solar radiation pressure model was unable to properly model the spacecraft in inertial pointing and Inner Cruise contingency mode orientations. Evidence to support our conclusion was found in the ADOR post-fit residuals, which fit much worse during inertial pointing than at any other time during cruise (see Figure 11c). Due to this model deficiency, it became standard procedure to estimate three-axis constant non-gravitational accelerations over the duration that thespacecraft entered these orientations. The duration of the non-standard orientations ranged from 16 hours to 8 days. The estimated acceleration components were on the order of 10^{-12} km/s**2, often smaller than the *a priori* 1-σ uncertainties of 1.0- 3.0x 10^{-12} km/s^2.

Geodetic Models

Two issues concerning geodetic models warrant elaboration in this report. First, a weekly change in the ADOR residuals was observed. These residuals split along the Spain-California and Australia-California baselines. Since no significant spacecraft event or change in orbit determination strategy were undertaken during these periods, it was hypothesized that the timing and polar motion arrays ('TP' arrays) were responsible for this change. Solutions were created, fitting all three data types, using TP arrays which contained different intervals of predicted polar motion information. Since Doppler data, and to a lesser degree range data, are sensitive to changes in polar motion. a TP array with poor polar motion information results in an offset trajectory for a solution dominated by Doppler data. This offset was revealed by the split baselines in the ADOR residuals. This baseline separation was exacerbated as more predicted polar motion data was used (see Figures 8a-b). Switching to more frequent TP array deliveries (twice a week instead of once a week) lessened the predicted polar motion data incorporated into orbit determination solutions. and the situation was ameliorated.

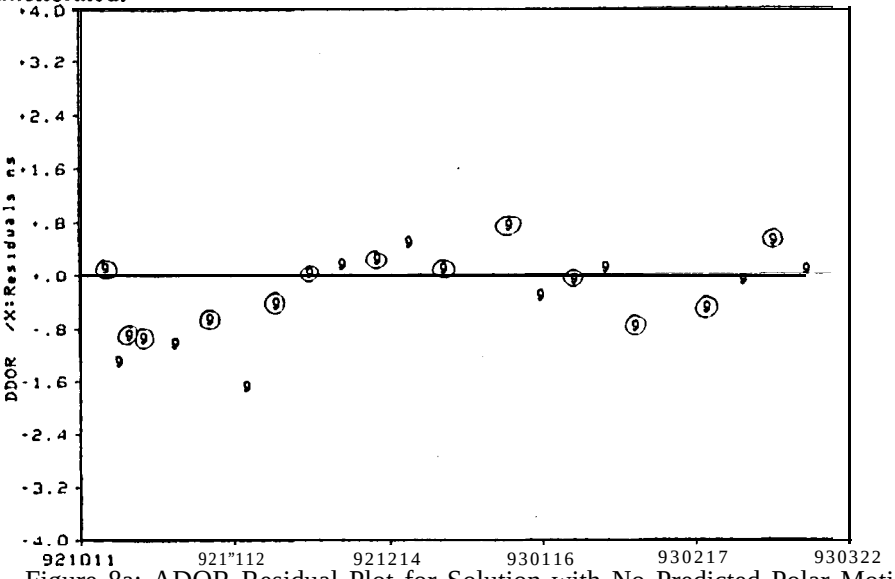

Figure 8a: ADOR Residual Plot for Solution with No Predicted Polar Motion
Circled Residuals: Australia-California baseline. Remaining points: Spain-California baseline

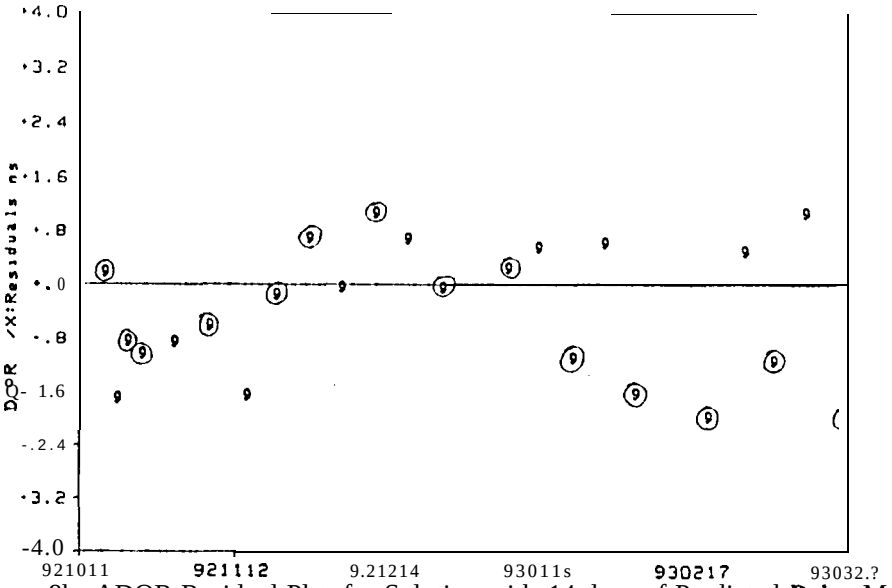

Figure 8b: ADOR Residual Plot for Solution with 14 days of Predicted Polar Motion
Circled Residuals: Australia-California baseline. Remaining points: Spain-California baseline

The second issue concerns the neglect of short period UT1 terms in the Launch version of the navigation software, which resulted in a change in the estimate of AMDs throughout cruise. These mismodeled AMDs introduced a 2-3 meter 'sawtooth' signature into the range residuals. An enhanced version of the navigation software, delivered in April 1993, incorporated the short period terms into the calculation of UT1. By re-estimating the AMDs with this model, the range residual signature was eliminated.

Filter Models

The standard filter configuration used during the MO cruise was of the single batch weighted least squares, square-root information type. No dynamic stochastic parameters were used in the orbit determination process. However, orbit solutions using stochastic range bias parameters with single diiy batches were made. No useful information was gained from the introduction of these parameters. As described in the Geodetic Models section, the range residual signature was removed by the introduction of the high frequency UTl terms and the subsequent re-estimation of the AMDs. The stochastic range biases only hid the range residual signature, and did not give insight as to the true nature of the mismodeling.

Table 4 lists the *a priori* uncertainties of parameters in the estimate and consider lists. and *a posterior* uncertainties from typical estimation results.

ORBIT DETERMINATION RESULTS

Significant solutions submitted during MO operations are presented. The quality of the orbit determination results are assessed in five manners. First, the solutions submitted for the backup and final MOI maneuver design provide an opportunity to assess the predicting capability of the MO cruise orbit determination (in lieu of a full cruise reconstruction). Second, from the experience accumulated from mission operations, one can identify and describe the predominant error sources in the solutions. Third, a battery of solutions using different data type combinations over the same orbit arc provided a check that all data types describe essentially the same trajectory. Fourth, solutions with different data arc lengths provided a check that our modeling capability is consistent throughout cruise. Finally, a comparison between pre-flight and actual orbit determination uncertainties demonstrated that the Mars Observer orbit determination met or exceeded its mission goals.

Orbit Determination Solution History

The sequence of designed Mars arrival points is described in detail in Reference 1. Table 5 and Figure 9 list the uncertainties in the arrival conditions during several stages of interplanetary cruise.

Table 4: **ESTIMATIO** AND CONSIDER PARAMETER MODELS

Estimated Parameters	*'A priori* Uncertainty (1σ)	A *posteriori* Uncertainty (1σ)
Spacecraft State at Epoch - Position	10,OCX). km	10.6 km (RSS)
Spacecraft State at Epoch - Velocity	1.0 km/s	4.0 mm/s (RSS)
Solar Radiation Pressure: Component Areas	4.5 - 9.3%	2.0% for solar array
Component μ, v (specular, diffuse coefficients)	10- 17.5?10 for large components	2.0%
Contingency Mode Accelerations	1.0- 3.0 x 10^{12} km/s^2	0.7- 1.4 X 10^{-12} km/s^2 (line-of-sight, -unobservable in plane-of-sky)
Angular Momentum Desaturation AV	1.0 mm/s	0.001 mm/s (line-of-sight, -unobservable in plane-of-sky)
Trajectory Correction Maneuver Model: AV (magnitude)	~2.0% (Variable, depending	0.5%
a (Rt. Ascension of Unit Thnrst Vector)	~1.3° on size of AV and	0.05"
δ (Declination of the Unit Thrust Vector)	~1.3° thrusters used.)	0.05"
Range Biases (One per station, constant across data arc)	10.0 50.0111	6.0- 30.0 m

Consider Parameters

Acceleration Bias: All Components	1.5- 2.0 x 10^{-12} km/s^2
DSS Locations (Correlated Covariance): Radial Distance	18. cm
Longitude	23. cm (at Earth's surface)
Z-height (height above true equator of date)	23. cm
UT1 - UTC	30.0 nrad
Earth GM	0,05 km^3/s^2
Moon GM	0.005 km^3/s^2
Mars GM	0.075-0.15 km^3/s^2
Earth J_2	1.0 x 10^{-8}
Mars J_2	1.1 X10-6
Mars Ephemeris (Epoch: MOI -5 days): Radial Position	0.16 km
Along-Track Position	5.6 km
Cross-Track Position	5.8 km
Absolute Quasar Location - *a*	5.0 nrad
Absolute Quasar Locations - δ	5.0 nrad
Zenith Troposphere	not considered
Zenith Ionosphere	not considered

Table 5: ARRIVAL STATE& UNCERTAINTIES DURING MO INTERPLANETARY CRUISE

Data Arc	Duration (Days)	B●T[a] (km)	B●R (km)	TCA[b] (Aug. 1993)	$\sigma_{B\bullet T}$ (km)	$\sigma_{B\bullet T}$ (km)	$V_{inf}\sigma_{TCA}$ (km)	Comment
9/27/92-9/30/92	3	-785982.	2104890.	10d 03:21:37	561.0	1462.0	2302.8	TCM- 1 Design
9/26/92- 1/27/93	123	217778.	-151449.	25d 03:18:42	368.2	290.0	223.8	TCM-2 Design
10/1 1/92-3/8/93	148	2522.	-4690.	24d 20:38:46	198.4	185.0	142.9	TCM-3 Design
9/26/92-6/14/93	261	-3.	-8380.	24d 20:40:56	34.1	43.2	32.5	Backup MOI Design
1/7/93-8/10/93	214	7.	-8397.	24d 20:40:06	9.5	17.8	11.4	Final MOI Design
1/7/93-8/22/93	226	7.	-8399.	24d 20:41:07	9.8	17.7	7.5	Final Solution

a. Planetary targeting is usually expressed in terms of the B-plane, a plane passing through the center of a target planet and perpendicular to the incoming approach hyperbola asymptote of a spacecraft, "B●T" is the intersection of the B-plane with the ecliptic and "B●R" is a 'southward' pointing vector in the B-plane that is perpendicular to B●T and making a right-handed system R, S, T, where S is the incoming asymptote.
b. TCA is the Linearized Time of Closest Approach. The Asymptotic Approach Velocity (V_{inf}) is 2.45 km/s.

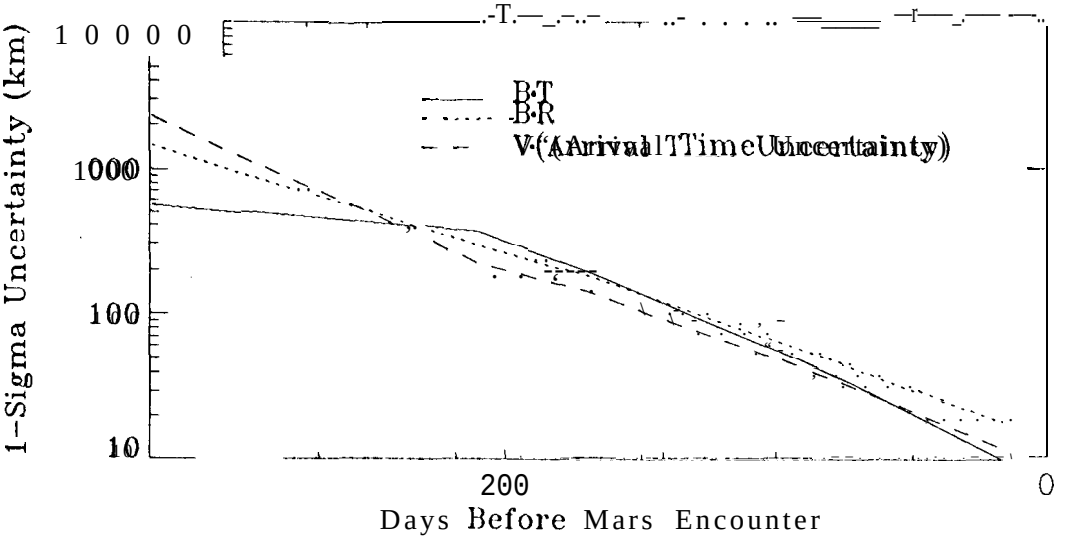

Figure 9: Arrival Condition Uncertainties Versus Time from Mars Encounter

Figure 10 depicts the orbit determination solution history from TCM-3 to the final MOI design. Solutions #1 - ##9 represent solutions submitted fortnightly to the project, Between Solutions #1 and #4 there were three changes in attitude due to contingency events (unscheduled attitude changes) which lasted several days. The net effect to the B-plane state was approximately a -100 km shift in B●T and a +20 km shift in B●R. Solution #6, submitted for the backup MOI design, is shown with its 1 -σ consider error ellipse*. Note that all solutions after the end of the contingency events (Solutions #4-9) are within this error ellipse, demonstrating that our error assessment was accurate.

In addition to submitting solutions for maneuver design, orbit determination analysts also reconstructed the three trajectory correction maneuvers (TCMs). Table 6 summarizes the maneuver reconstructions (in right ascension (a), declination, (δ), and magnitude (ΔV)) and the nominal values for each maneuver.

*This solution was also submitted for the Mars Observer Camera (MOC) sequence, which resulted in the only Mars images of the mission.

Table 6: CRUISE TCM NOMINAL VALUES AND NAVIGATION RECONSTRUCTIONS

	TCM-1		TCM-2		TCM-3	
Parameter	Nominal	Reconstruction	Nominal	Reconstruction	**Nominal**	Reconstruction
a (deg)	-123.755	-125.075	198.286	196.598	-93.890	-94.668
δ (deg)	-15.193	-15.373	-17.6131	-20.132	54.621	54.914
ΔV (m/s)	50.005	50.005	9.6508	9.662	0.466	0.4611
o(a) (deg)	1.3188	0.0001345	1.3755	0.021	0.6965	0.052
σ(δ) (deg)	1.2729	0.0009182	1.3110	0.050	0.4035	0.092
σ(ΔV) (111/S)	1.009	0.0001	0.0254	0.003	0.00377	0.0030

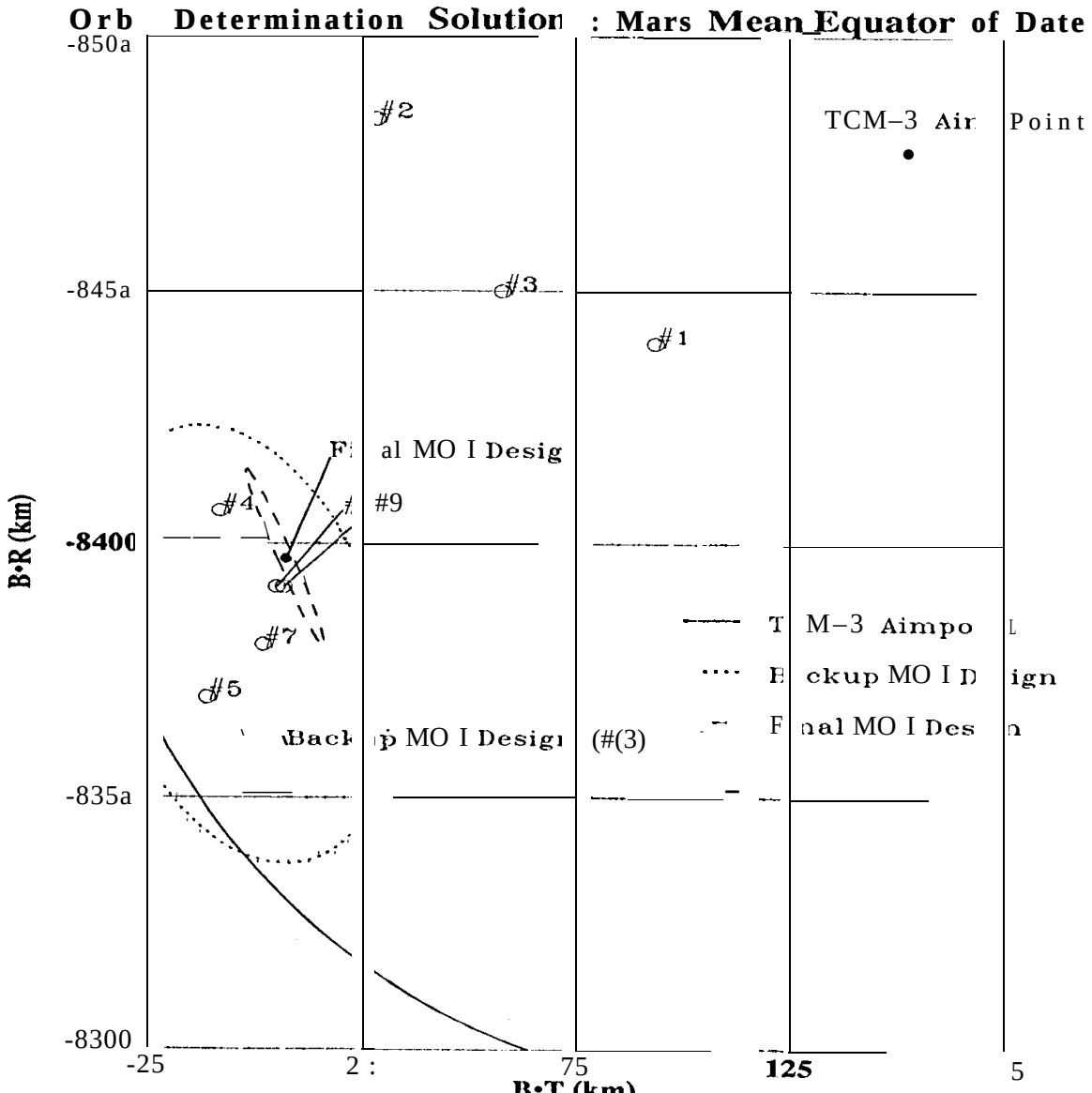

Figure 10: B-Plane **Locations of Post-TCM-3** Solutions
(including those submitted for Backup and Final **MOI** Design)

Data Quality

The MO navigation team received unedi ted Doppler and range tracking data via the Radiometric Data Conditioning Team (RMDCT) once per working day. The orbit determination analysts noted problems with the Doppler and range tracking data. Reports were submitted which described the following problems:

(1) Doppler data from Canberra would include blunder points with a constant bias several hundred Hertz in magnitude.

(2) Doppler data from Goldstone would display signatures whose amplitude was greater than the data noise, sometimes an order of magnitude greater.

(3) Range data from entire passes from every station would occasionally display blunder points and biases.

(4) Range data from Canberra during the middle of pass would add a large bias for a round-trip light time, then return to a normal signature,

Of these problems, the range problems were better understood. The episodes described in (3) were found to coincide with switches from 4 kb/s to 8 kb/s telemetry. This change reduced the ranging channel power by over 12 dB. Early in cruise, the ranging power margin was in the tens of dB, so this problem was not revealed until the outer cruise phase. The Canberra range bias problem was found to be caused by a mal - functioning receiver / exciter controller (REC) digitally controlled oscillator (DCO) at that station. The Doppler data problems were due to time tag problems from the implementation of the new Metric Data Assembly (MDA) software at the stations. From data taken during the first half of June 1993,91 of 1299 Doppler points and 383 of3914 range points were deemed unusable, corresponding to failure rates of 7.0 and 9.8 percent, respectively. While these losses did not affect the quality of the cruise orbit determination, losses of this magnitude could have affected the orbit determination during the orbit insertion and mapping phases at Mars, so they were reported to the project.

In addition to these problems, there were occasional signatures in the Doppler data when the angular speed in the spacecraft reaction wheels passed zero. The signature (according to telemetry from the spacecraft team) was a decaying sinusoid with a period and decay constant of approximately 3 minutes each. This signature was observed when the navigation team requested Doppler data every 10 s. However, since most orbit determination work was performed with 10 minute data, this signature was not observed, and no compensations were made to the observable.

The scatter in the post-fit residuals (see Table 7 and Figures 12a-e) was consistent throughout cruise with the exception of the range data, whose residual scatter varied as the spacecraft-Earth distance increased and the range integration times were changed. In a Doppler-only solution, the range data would contain a bias on the order of hundreds of meters; this was considered acceptable given the state position uncertainty of 1-2 km.

Table 7: MEASUREMENT ***A PRIORI*** UNCERTAINTIES&A ***POSTERIORI*** RESULTS

Data Types Fitted in Solution	Data Type	*A priori* Weighting (1 -σ)	*A posteriori* RMS residuals (1-σ)
Doppler, Range, ADOR	Doppler	10 mHz (0,2 mm/s)	1 mHz (0.02 mm/s)
	Range	10 meters	1-2 meters
	ADOR	1.0 ns (80 nrad)	0.6 ns (50 nrad)
Doppler Only	Doppler	10 mHz (0.2 mm/s)	1 mHz (0.02 mm/s)
	Range	N/A	100-400 meters
	'ADOR	N/A	1.0 ns (80 nrad)

Final B-Plane Uncertainties

For the solution submitted for the final MOI design, uncertainties of all estimated and considered parameters were mapped to the encounter epoch. The largest uncertain y by far came from the Mars planetary ephemeris. There was no clear ranking of the uncertainties associated with the remaining parameters.

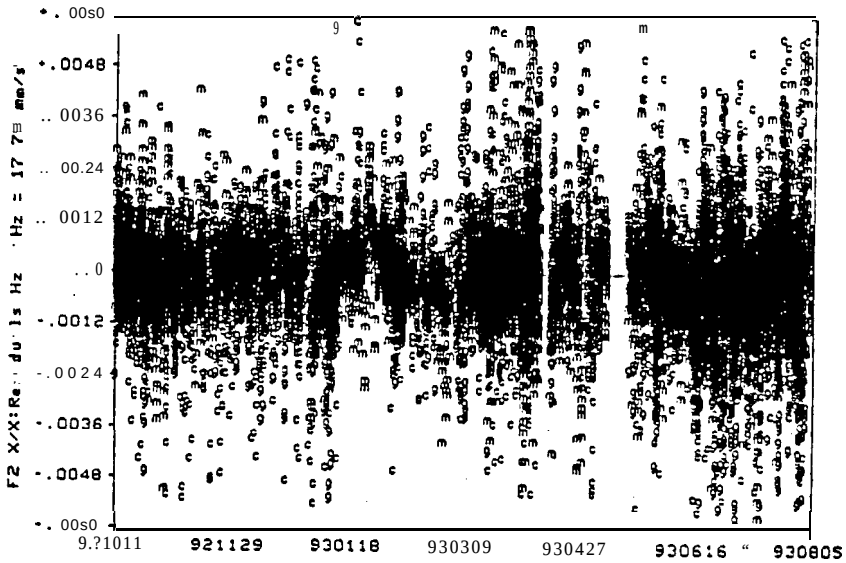

Figure ha: Typical Data Residuals For Fitted Doppler Data
(18985 points, Mean = **0.028 mHz, 1-σ** Scatter= 1.1S **mHz)**

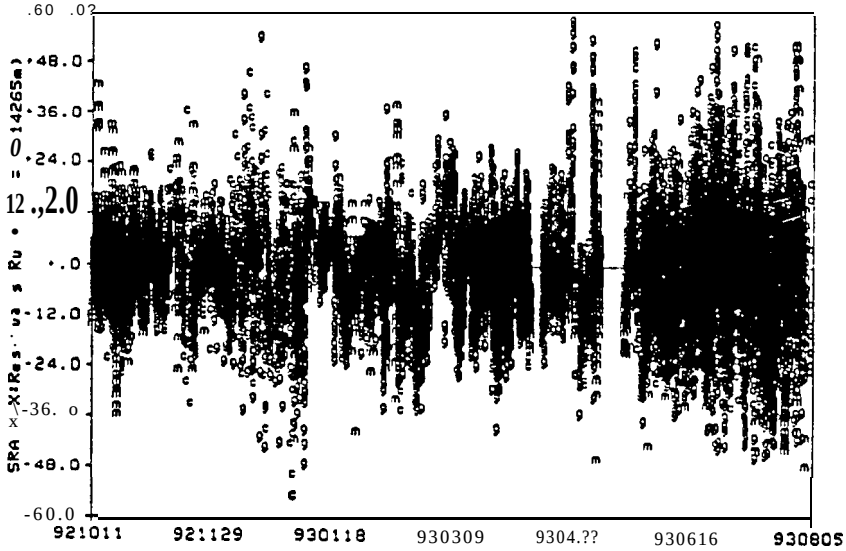

Figure 11b: Typical Data Residuals For Fitted Range Data
(24026 points, Mean = 0.069 Range Units, **1-σ** Scatter = 11.1 Range Units)

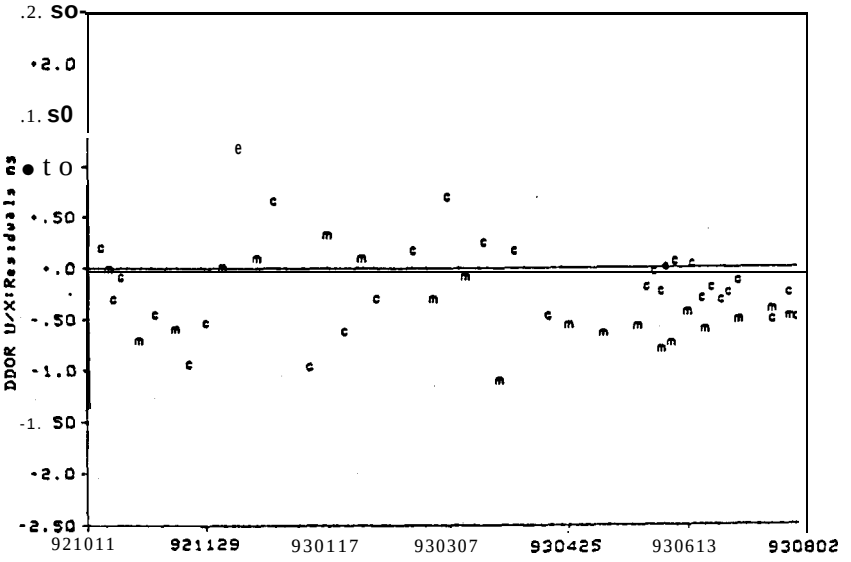

Figure IIc: Typical Data Residuals For Fitted ADOR Data
(52 points, Mean = 0.233 ns, 1-σ Scatter= 0.426 ns)

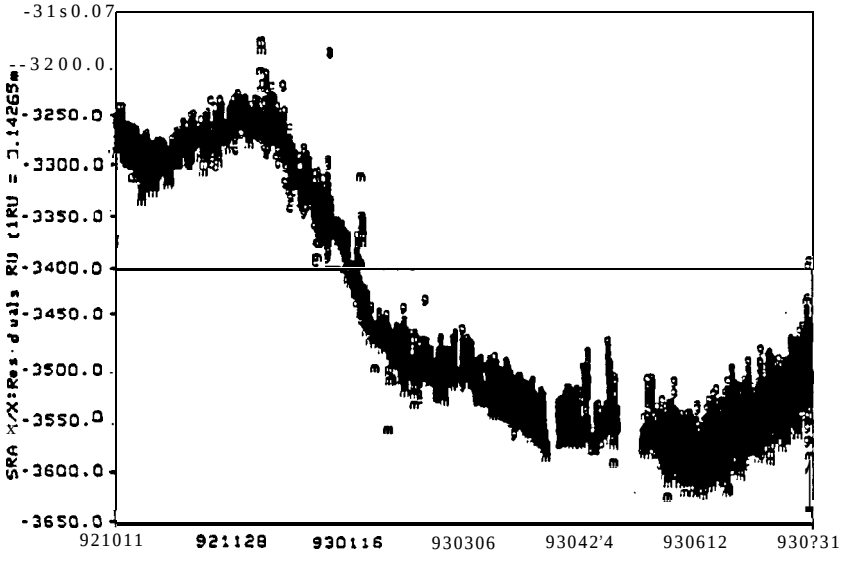

Figure IId: Typical Data Residuals For Range Data Passed Through a Doppler-Only Solution (23961 points, Mean = -3468. Range Units, 1-σ Scatter = 115. Range Units)

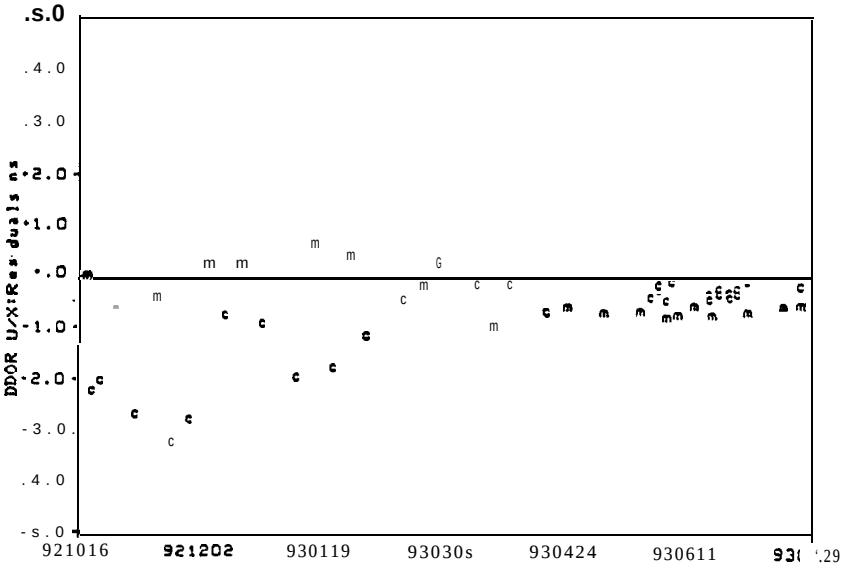

Figure he: Typical Data Residuals For ADOR Data Passed Through a Doppler-Only Solution
(50 points, Mean = -0.58 ns, 1-σ Scatter= 0.S42 ns)

Backup & Final OD Solution Comparison

A solution was submitted for the backup MOI design 57 days prior to the submission of the final MOI design solution (see Figure 10). To check the predictive accuracy of the former solution, data collected between the creation of these two solutions was passed through the backup MOI solution. Values for AMD events after the data cutoff of the backup solution were added to the pass-through for consistency, The final discrepancy in Doppler and range residuals was found to be 1.0 mm/s and 0.6 km, respectively (see Figures 12a-b).

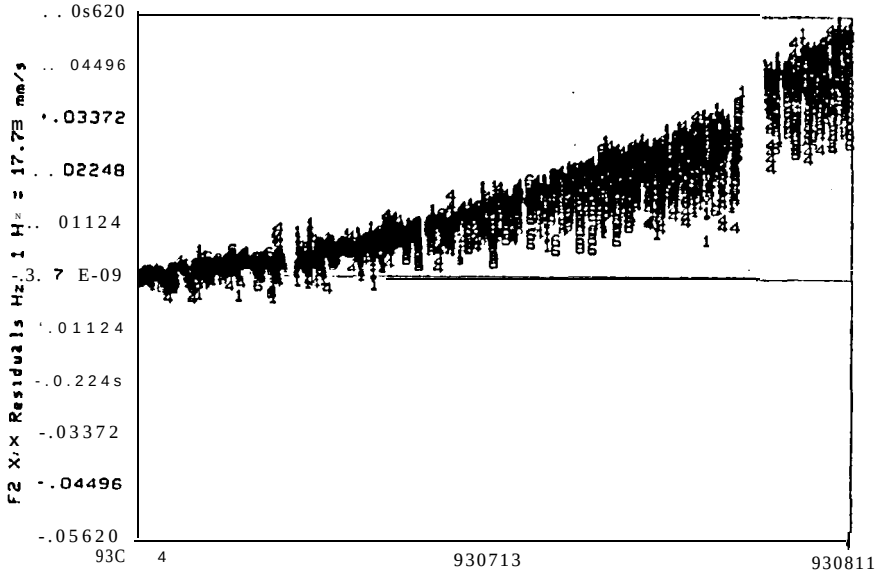

Figure 12a: Cruise Doppler Data Passed Through the 'Backup' MOI Solution
(5319 points, Mean = 17.1 mHz, 1-o Scatter= 14.2 mHz)

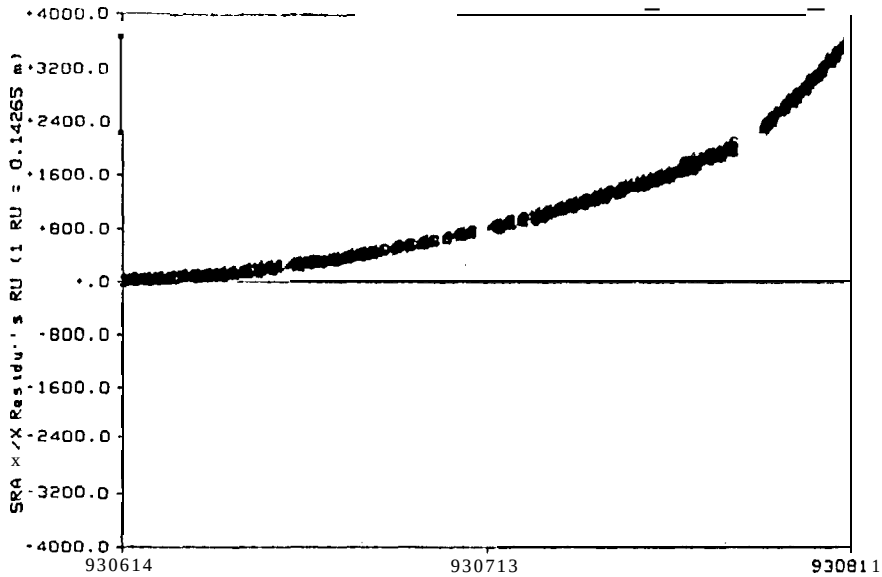

Figure 12b: Cruise Range Data Passed Through 'Backup' MOI Solution
(5004 points, Mean =1175. Range Units, 1-σ Scatter = 1009. Range Units)

Variation by Data Type Combination

The availability of three radiometric data types during cruise made it possible to perform orbit determinations using different combinations of data types. The standard procedure was to first create a Doppler-only solution, since from experience Doppler is the most trusted data type. Range and ADOR data were passed through this solution in order to assess their quality. Second. a Doppler-Range solution was created. As additional range data was passed through a Doppler-Range solution after an AMD event, the orbit determination analyst could estimate the timing of the event if it occurred outside a tracking pass. Next, the ADOR data was introduced to create a third solution. Other data combination types (Range-ΔDOR, Doppler-ADOR) were also created. Figure 13 depicts the B-plane locations for a battery of solutions which have the same data arc as the solution submitted for the final MOI design.

Though each solution used a different combination of data types, they all fell within the final MOI design solution's 1-σ consider error ellipse (shown). Conversely, the error ellipses associated with each solution contain the B-plane point of the solution submitted for the final MOI design (these error ellipses are not shown for clarity). All data type combinations are consistent within 1 -σ in the MOI arrival time and location.

Variation by Arc Length

Figure 13 also shows solutions with two different data arc lengths, the solution submitted for MOI design (215 day data arc) and a short arc solution (24 day data arc). The short arc solution is within 1.5-0 of the former solution. Longer arc solutions (up to 330 days) agreed with the submitted solution to less than 1 -cr. The solution labeled 'final receipt of data' is the closest solution to a full trajectory reconstruction available. This solution is also consistent with all of the other solutions displayed.

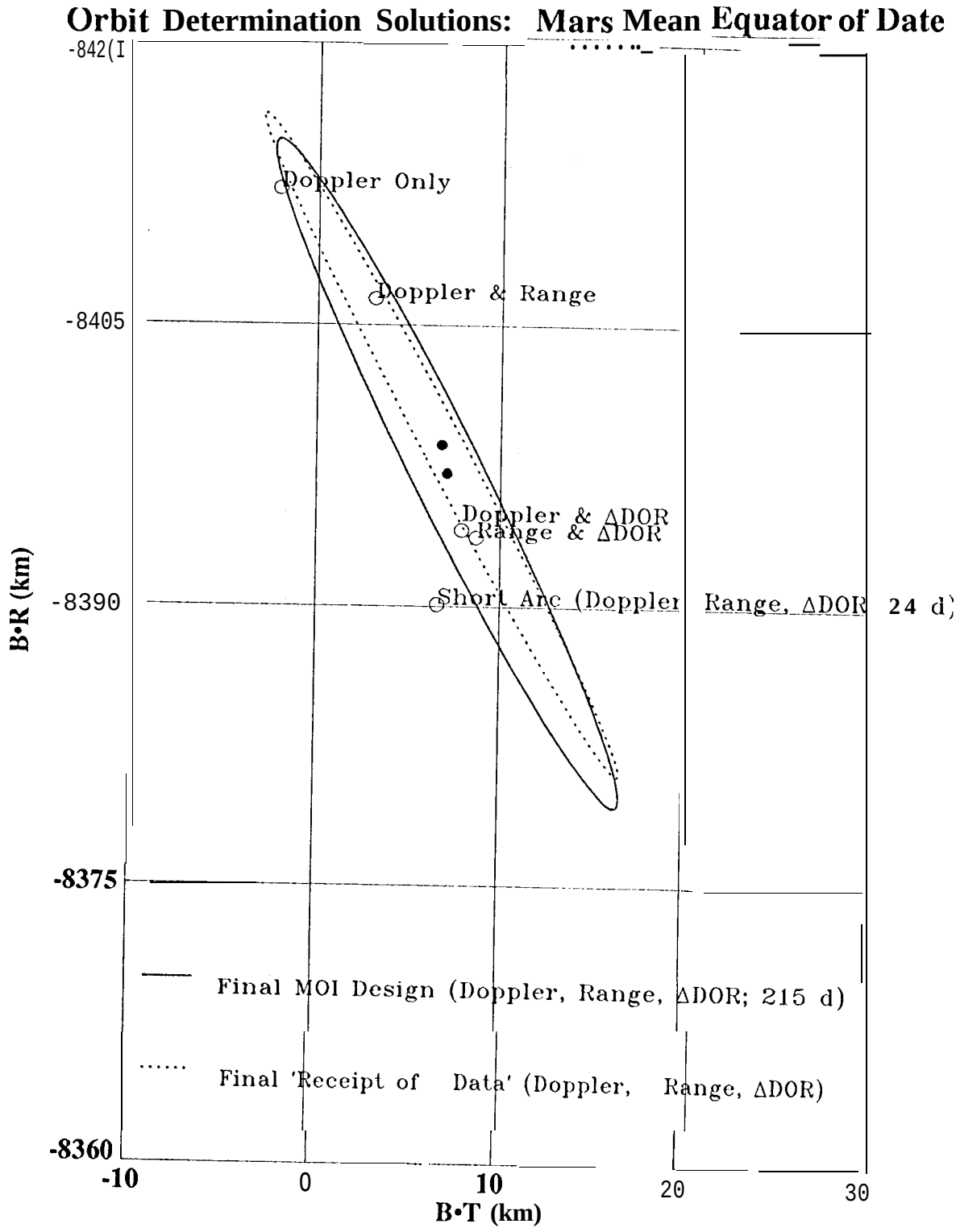

Figure 13: B-Plane Locations for Solutions Varying by Data Type Combination and Data Arc Length

Predicted vs. Actual Orbit Determination Performance

B-plane uncertainties in typical orbit determination solutions at the end of cruise were compared to predicted uncertainties calculated early in the cruise phase. Table 8 shows a comparison of predicted and actual uncertainties for solutions with a data cutoff of MOI-25 days. The actual uncertainties are smaller than those predicted for two reasons. First, it was contemplated that stochastic attitude control parameters might have been needed during cruise; this was found not to be the case. Second, the acceleration bias included in the consider analysis was lowered from a pre-launch estimate of 3.0 x 10-]2 km/s^2 to values of 1.5-2.0 x 10^{-12} km/s^2.

Table 8: 1-0 ORBIT DETERMINATION PERFORMANCE (MOI-25 DAYS)

B-Plane	Semi-major Axis (km)	Semi-minor Axis (km)	θ (deg)	Linearized Time of Flight (s)
Predicted	24.5	5.1	63.8	12,1
Actual	19.4	2.0	63.8	5.1

CONCLUSIONS

Operations teams design their activities to maximize spacecraft safety and team efficiency. The Mars Observer navigation team focus was on the successful delivery of navigation assessments and products to the project. These goals were achieved, and in that process several conclusions were reached by the team of orbit determination analysts.

All the models employed in the orbit determination process were found to be adequate for the navigation precision required by the project. The greatest model limitation was the inability to describe the spacecraft in non-standard orientations in the solar radi at ion pressure model, The greatest contribution to the B-plane uncertain y for the final solutions came from the Mars planetary ephemeris. All three data types (Doppler, range, and ADOR) fit at levels equal to or better than project requirements. All orbit determination solutions were consistent with subsequent solutions, and were consistent across different data type combinations and data arc lengths. The quality of the radiometric data, which was better than expected, allowed this consistency to be seen, but the consistency was achieved through the development of an accurate and realistic set of models.

ACKNOWLEDGMENTS

The work described in this paper was carried out at the Jet Propulsion Laboratory, California Institute of Technology, under a contract with the National Aeronautics and Space Administration. The Mars Observer project was managed for the National Aeronautics and Space Administration by the Jet Propulsion Laboratory, California Institute of Technology. The fellow members of the Mars Observer navigation team, W. E. Bollman, C. M, Diarra, C. A, Halsell, and M. D. Johnston were integral to the MO navigation operations described in this report. The authors would like to acknowledge J. S. Border for his assistance in interpreting the ADOR results. The authors would also like to thank J. Ellis and T. P. McElrath for an informal review of the manuscript.

REFERENCES

[1] P. B. Esposito, W. G. Bellman, *et al*, "Navigating Mars Observer: Launch Through Encounter and Response to the Spacecraft's Pre-Encounter Anomaly," AAS 94-119, AIAA/AAS Space Flight Mechanics Meeting, Cocoa Beach, FL, 14-16 February 1994,

[2] Mars Observer Navigation Team Final Report, JPL Interoffice Memorandum NAV-93-183, 29 December 1993.

[3] E. Graat, D. Roth, "Mars Observer Launch Lockfile Version 3,0," JPL Interoffice Memorandum NAV-92-081, 15 September 1992.